ANTIOXIDANTS & REDOX SIGNALING
Volume 12, Number 3, 2010

DOI: 10.1089/ars.2009.2814

Edaravone Inhibits Protein Carbonylation by a Direct Carbonyl-Scavenging Mechanism: Focus on Reactivity, Selectivity, and Reaction Mechanisms

Giancarlo Aldini, Giulio Vistoli, Luca Regazzoni, Maria Carmela Benfatto, Ilaria Bettinelli, and Marina Carini

Abstract

The aim of this study was to evaluate the ability of the well-known radical scavenging compound edaravone (EDA) to entrap and detoxify reactive carbonyl species (RCS) derived from lipid peroxidation [4-hydroxy-*trans*-2-nonenal (HNE), acrolein and glyoxal], as well as its ability to prevent RCS-induced protein carbonylation, by using hemoglobin (Hb) modified by HNE as an *in vitro* model. Through a combined HPLC and high-resolution mass spectrometric approach, we confirmed the ability of EDA to scavenge precursors for either advanced glycation or lipoxidation end products (EAGLEs), such as glyoxal, and demonstrated for the first time that EDA is also a potent quencher of α,β-unsaturated aldehydes (providing mass spectral characterization of the adducts), being significantly more active than a series of well-known RCS sequestering agents. Direct infusion analysis of the intact protein and nano LC-ESI-MS/MS analysis of the tryptic digest, carried out on an LTQ-Orbitrap hybrid mass spectrometer, were used to study the modifications occurring on Hb after exposure to increasing HNE concentrations, providing evidence for Cys93 (Hb β-chain) involvement in covalent attachment, and to demonstrate the ability of EDA dose-dependently to inhibit Hb carbonylation. Computational studies allowed us to elucidate the mechanism of EDA-RCS interaction and to explain the preferential site of HNE adduction to Hb. The same combined approach indicated that EDA is not a selective RCS scavenger, being able to react also with nontoxic, physiologically relevant aldehydes, such as pyridoxal. *Antioxid. Redox Signal.* 12, 381–392.

Introduction

Much evidence indicates that oxidative stress plays a crucial role in aging as well as in neurodegenerative, cerebrovascular, and cardiovascular diseases. It is now well accepted that oxidative damage, besides being induced and propagated by free radicals, is also mediated by the formation of oxidation-derived reaction products, such as lipoxidation-derived reactive carbonyl species (RCS). RCS, by inducing covalent modifications (cross-linking) of functional and structural proteins, trigger key cell-signaling and protein inactivation. The loss of function or structural integrity of proteins by RCS attack can have a wide range of downstream functional consequences, and for this reason, carbonylated proteins are well-recognized signs of cell and tissue damage (2, 10, 20, 24). Protein carbonylation constitutes one of the best-characterized biomarkers of oxidative stress and oxidative damage in several conditions and diseases, and the availability of a number of robust and accurate methods, including redox proteomics and mass spectrometry technologies, greatly facilitated, in the last few years, the detection and quantification of protein-bound carbonyls in cells, tissues, and body fluids (2, 4–6, 8, 9). Furthermore, a strict correlation between carbonyl stress and certain human diseases is now well established (10), such as in the case of diabetes-related diseases (23), age-dependent tissue dysfunction (19), neurodegenerative diseases (15), and atherosclerosis (27). Consequently, RCS not only are predictive biomarkers of oxidative damage, but also represent new biologic targets for drug discovery (1, 17).

Taking RCS and carbonylation damage as a drug target, the first molecular strategy considered to neutralize/reduce these pathogenetic factors was based on free radical scavengers that prevent lipid peroxidation by capturing highly reactive oxygen species (ROS). As an alternative strategy to the antioxidant approach, several efforts have been made in the last few years to discover efficient RCS scavengers, nucleophilic compounds able to entrap highly electrophilic,

Dipartimento di Scienze Farmaceutiche "Pietro Pratesi," Università degli Studi di Milano, Milan, Italy.

highly cytotoxic lipid-derived RCS (identified as the chemical intermediates between hyperglycemia, hyperlipidemia, and their complications), and to detoxify them by forming covalent and unreactive adducts (RCS-sequestering agents) (1, 2, 17).

In other words, the first compounds might prevent the RCS formation, whereas the last ones might neutralize the RCS effects, avoiding their accumulation. The nonenzymatic antioxidants normally include reducing compounds (ascorbic acid, α-tocopherol, carotenoids, and flavonoids) which are able to capture one electron, whereas reactive carbonyl scavengers typically involve nucleophilic compounds (histidine-containing dipeptides, aminoguanidine, and hydralazine), able to form covalent products with RCS mainly through Michael-type addition. Usually, the investigated molecules do not combine both effects, even if a very important exception is represented by endogenous glutathione (GSH) whose sulfhydryl group can act as a nucleophile or reducing agent or both, being oxidized into the corresponding disulfide homodimer (GSSG). Another promising molecule that may combine the two mentioned mechanisms is edaravone (MCI-186, 3-methyl-1-phenyl-2-pyrazolin-5-one), whose activity is truly original, being based on the acidity of the methylene group in α to a carbonyl function.

Edaravone (EDA) is a well-known free radical scavenger that has been shown to have protective effects against cerebral ischemia/reperfusion injuries in a variety of experimental animal models. The clinical efficacy of edaravone against ischemic brain attack has been demonstrated by the presence of significant improvements in functional outcome in a randomized, placebo-controlled, double-blind study, and indeed, it has been approved by the Japanese health authorities as a neuroprotective agent for the treatment of acute cerebral infarction since 2001.

In addition to these antistroke effects, edaravone has been shown to prevent oxidative damage to various extracerebral organs (29) and to inhibit accumulations of HNE and 8-hydroxy-deoxyguanosine, which are oxidative byproducts, as well as neuronal cell death after transient focal ischemia in the murine brain (32). Systemic administration of edaravone attenuates the increase of malondialdehyde levels, the reduction of superoxide dismutase (SOD) activity, and suppresses the retinal dysfunctions after retinal ischemia/reperfusion in rats, as well as oxidative stress-induced endothelial damage and early atherosclerosis in ApoE-KO mice (30). More recently, the screening of a large chemical library disclosed that edaravone inhibits *in vitro* the advanced glycation end product (AGE) formation efficiently (14), by trapping both reactive carbonyl compounds (glyoxal and methylglyoxal) precursors for EAGLEs and AGEs, respectively.

Although the mechanisms for radical scavenging of EDA were deeply explored with several approaches, little or nothing has been done to investigate the precise mechanisms by which the compound can react with toxic and nontoxic physiologically relevant carbonyl compounds. Because generation of drugs sharing both antioxidant and carbonyl scavenger properties represents a new therapeutic challenge in the treatment of carbonyl stress-associated diseases, this study was undertaken to gain a deeper insight into the RCS trapping ability of EDA, and in particular, (a) experimentally to confirm, by an unequivocal mass-spectrometric approach, the reactivity toward carbonyl compound precursors of EAGLEs; (b) to evaluate its potency as a scavenger of highly reactive and cytotoxic lipid-derived α,β-unsaturated aldehydes (HNE and acrolein), precursor of ALEs (advanced lipoxidation end products), never considered; (c) to unveil mechanisms, stoichiometry, and reaction products of EDA with both toxic and endogenous (pyridoxal) aldehydes; and (d) to demonstrate the ability of the compound to prevent/inhibit protein carbonylation, by using RCS-modified hemoglobin as an *in vitro* model.

Materials and Methods

Chemicals and reagents

Human hemoglobin (Hb), hydralazine (HY), pyridoxamine (PYR), pyridoxal (PYAL), acrolein (ACR), and glyoxal (GO) were purchased from Sigma-Aldrich (Milan Italy). Because Hb was predominantly methemoglobin, before use, it was dissolved in 2 m*M* Tris–HCl (pH 7.5), reduced by 1,4-dithioerythritol (DTE, 0.5 m*M*), and then dialyzed overnight with Milli-Q water. Edaravone (3-methyl-1-phenyl-2-pyrazolin- 5-one; EDA) was from Tocris Bioscience (Bristol, U.K.). 4-Hydroxy-non-2-enal diethylacetal (HNE-DEA) was synthesized according to the literature (23). 4-Hydroxy-*trans*-2-nonenal (HNE) was prepared from HNE-DEA with 1 m*M* HCl hydrolysis (1 h at room temperature) and quantified with UV spectroscopy (λ max, 224 nm; ε, 13,750 l mol/cm). Carnosine (β-alanyl-L-histidine, L-CAR), was a generous gift from Flamma S.p.A (Chignolo d'Isola, Bergamo, Italy). LC-MS–grade solvents, Chromasolv, were purchased from Sigma-Aldrich. Sequence-grade modified trypsin was obtained from Promega (Milan, Italy). LC-grade water (18 mΩ) was prepared with a Milli-Q water-purification system (Millipore, Bedford, MA). All other reagents were of analytic grade.

Protein carbonylation: MS studies

Sample preparation. HNE-induced carbonylation of Hb was studied by incubating 20 μ*M* Hb solution with HNE at different molar ratios (Hb/HNE, 1:1; 1:5; 1:10) in 1 m*M* phosphate buffer (pH 7.4) for 120 or 240 min at 37°C. The dose-dependent effect of EDA on Hb carbonylation was studied by co-incubating for 120 min 20 μ*M* Hb in the presence of 200 μ*M* HNE at different EDA doses (40, 200, and 400 μ*M*).

Direct infusion mass spectral analysis. To detect changes in the protein mass of the α- and β-globin subunits, samples prepared as described earlier were analyzed with direct infusion into a LTQ-Orbitrap Hybrid Mass Spectrometer (Thermo Scientific, Milan, Italy) equipped with an Electrospray Finnigan Ion Max source. Aliquots (50 μl) of each sample were mixed with 150 μl of H_2O:CH_3CN:HCOOH (50:50:0.1, vol/vol/vol), infused into the mass spectrometer at a flow rate of 3 μl/min and analyzed in full-scan mode, under the following instrumental conditions: AGC target, 5×10^4; 500-ms maximum inject time; one microscan, scan time, 1.9 s; resolving power, 100,000 positive ion mode; capillary temperature, 270°C, spray voltage applied to the needle, 3.5 kV; capillary voltage, 37 V; nebulizer gas (nitrogen) flow rate set at 5 (a.u.); acquisition time, 1 min. Direct infusion ESI-MS spectra were deconvoluted by using Xtract for Qual Browser v. 2.0.7 (ThermoQuest).

Nano LC-ESI-MS/MS analysis. The HNE-induced structure modifications of Hb were characterized with nano LC-ESI-MS/MS analysis of incubated samples after reduction with $NaBH_4$, an established procedure for adduct stabilization (7, 12), followed by enzymatic digestion, by using trypsin as proteolytic enzyme and iodoacetamide as an alkylating agent. Peptide mass mapping provided identification of the peptides, accounting for ~96% of the protein sequence. All digested peptide mixtures were separated with online reversed-phase (RP) nanoscale capillary liquid chromatography (nanoLC) and analyzed with electrospray tandem mass spectrometry (ESI-MS/MS). Chromatography was performed by using a Surveyor LC system (ThermoFinnigan Italia, Milan, Italy) on a 180-μm×10-cm column packed with a 5-μm, Biobasic-18 stationary phase (Thermo, Superchrom, Milan, Italy). The pump flow rate was split 1:75 for a column flow rate of 1 μl/min. The column effluent was directly electrosprayed by using the silica emitter source without further splitting. Solvents A (water containing 0.1% HCOOH) and B (methanol containing 0.1% HCOOH) were used as a mobile phase. The separation of tryptic peptides was achieved by gradient elution from 0 to 100% B over a 65-min period. Before the next analysis, both the precolumn and the column were first washed with 100% solvent B for 10 min and then equilibrated with 100% solvent A for 20 min. For the identification of peptides, an LTQ XL-Orbitrap mass spectrometer was used (Thermo Scientific, Milan, Italy) and the electrospray interface (dynamic nanospray probe; Thermo Scientific) was set as follows: spray voltage, 1.6 kV; capillary temperature, 220°C; capillary voltage, 30 V; tube lens offset, 120 V, and no sheath or auxiliary gas flow. The analyses were performed in positive polarity enabling the data-dependent scan mode. The MS spectra were acquired in profile mode by Orbitrap in the following conditions: scan range, 250-2,000 m/z in full-scan mode with full-scan injection waveforms enabled; AGC target setting, 5×10^5; maximum inject time, 500 ms; scan time, 1 s (60,000 resolving power at 400 m/z, FWHM). A list of 14 protonated phthalates and siloxanes including dibutylphthalate (plasticizer, m/z 279.159086); bis(2-ethylhexyl)phthalate (m/z 391.284286) and dodecamethylcyclohexasiloxane $[(Si(CH_3)_2O)_6 + H]^+$; m/z 445.120025] were used for real-time internal mass calibration (19). Tandem mass spectra were recorded by the linear ion trap in centroid mode for the three most intense ions (isolation width, 2 m/z; normalized collision energy, 35 CID arbitrary units; minimum signal threshold, 5×10^4), and dynamic exclusion was enabled (repeat count, three; repeat duration, 10 s; exclusion-list size, 25; exclusion duration, 120 s; relative exclusion mass width, 5 ppm). Charge-state screening and monoisotopic precursor selection was enabled, singly and unassigned charged ions were rejected.

HNE adduct identification. The acquired MS/MS spectra were searched by using the Bioworks software (rev. 3.3.1 sp1; Thermo Scientific) and by using a database containing only the protein of interest. The following settings were used for the search engine: mass type, monoisotopic precursor and fragments; enzyme, trypsin (KR); missed cleavage sites, 5; peptide tolerance, 5 ppm; fragmentations tolerance, 0.5 AMU; modifications, 5 PTMs per peptide; the variable modifications considered were as follows: HNE reduced Michael adduct to His, Lys, and Cys (+158.13067 Da as monoisotopic mass); reduced HNE Schiff base with the ε amino group of Lys (+140.12011 Da as monoisotopic mass); and fixed modification: carbamidomethylation on Cys. Results were filtered by setting the peptide probability to 0.005.

Reactivity and selectivity

HPLC studies. The reactivity of EDA and of the reference compounds toward different RCS (scavenging activity) was evaluated by measuring their consumption (50 μM in 10 mM PBS, pH 7.4) in the presence of the tested compound (1 mM) at a fixed incubation time (180 min, T = 37°C). HNE and ACR consumption were determined by HPLC, using a quaternary pump HPLC system and a PDA detector (Surveyor LC system; ThermoQuest) set at 224 nm. Separations were done by reversed-phase elution with a Phenomenex Synergy Fusion column (150 mm × 2 mm i.d., 4 μm) protected by a Synergy Fusion R-P guard column (CPS Analitica, Milan, Italy), thermostated at 37°C, and using H_2O:CH_3CN:HCOOH (50:50:0.1; vol/vol/vol) as mobile phase at a flow rate of 0.25 ml/min. GO consumption was determined after derivatization with *o*-phenylendiamine according to Miyata *et al*. (16).

Selectivity was determined in a similar manner after 180-min incubation, by using PYAL as a target physiologically relevant aldehyde. PYAL consumption was determined with HPLC by using a fluorimetric detector, as previously reported (16). The results are reported as percentage of the free aldehyde remaining with respect to a blank, incubated in the absence of the tested compound.

Direct-infusion MS experiments. Structure characterization of the adducts was determined with MS studies (direct infusion) on a triple-quadrupole (TQ) mass spectrometer (Finningan TSQ Quantum Ultra, ThermoQuest) equipped with an Electrospray Ion Max source at a flow rate of 10 μl/min. Samples were prepared by incubating for 180 min 0.5 mM EDA in 1 mM phosphate buffer (pH 7.4) with an equimolar concentration of the target aldehyde (HNE, ACR, and PYAL in 1 mM phosphate buffer, pH 7.4). An aliquot of the mixture was then diluted 1:4 (vol/vol) with H_2O:CH_3CN (70:30; vol/vol) and analyzed with direct-infusion MS. Mass spectrometric analyses were performed in positive ion mode. ESI interface parameters were set as follows: middle position; capillary temperature, 270 °C; spray voltage, 4.0 kV. Nitrogen was used as the nebulizing gas at the following pressure: sheath gas, 30 psi; and auxiliary gas, 5 a.u. For each compound tested, the most suitable instrumental conditions were searched for by using the Quantum Tune Master software (Thermo Scientific, Milan, Italy). Elemental composition of each reaction product was determined on the basis of exact mass measurements (resolution, 100,000) obtained with direct infusion on an LTQ XL-Orbitrap hybrid mass spectrometer (Thermo Scientific) equipped with an Electrospray Finnigan Ion Max source by using a list of 14 protonated phthlates and siloxanes, including dibutylphthlate (plasticizer, m/z 279.159086); bis(2-ethylhexyl) phthalate (m/z 391.284286) and dodecamethylcyclohexasiloxane $[(Si(CH_3)_2O)_6 + H]^+$; m/z 445.120025] for real-time internal mass calibration (19).

Molecular formulas were generated by the Elemental Composition feature included in Xcalibur Qual Browser 2.0 (Thermo Scientific) by following the rules described by Kind and Fiehn (26). The maximum error of mass measurements

was set at 5 ppm; the nitrogen rule and a restriction for carbon atoms in each formula were applied, considering a 5% relative error in the $^{12}C/^{13}C$ isotope ratio measurements.

Computational details

Docking studies. The different abundance of the HNE-Hb adducts was investigated *in silico* by docking the HNE molecule into the experimentally resolved structure of hemoglobin (PDB Id: 1 HGC). Specifically, the retrieved protein structure was completed by adding the hydrogen atoms. At physiologic pH, Arg, Lys, Glu, and Asp residues were preserved ionized, whereas His and Cys residues were considered neutral by default. The structure underwent a global minimization with backbone atoms and heme groups fixed to preserve the experimental folding. The obtained hemoglobin structure was then exploited in docking calculations by using the Biodock program (22), which performs a fully blind search, randomly rototranslating the HNE structure over the entire hemoglobin surface. In detail, Biodock produced 1,000,000 possible poses clustered in ~5,000 nonredundant solutions that were scored according to the CVFF non–bond-interaction energy. The best docking result around Cys β93 was finally minimized, keeping the atoms fixed outside 15 Å around the docked HNE molecule to preserve the hemoglobin structure. All mentioned minimizations were carried out with Namd2.51 by using the conjugate gradient algorithm until RMS = 0.01.

Reactivity analyses. To rationalize the scavenging activity of edaravone toward ACR and HNE, the reactivity of the reported adducts was analyzed by calculating the molecular softness that is a quantum mechanical index of the global reactivity toward nucleophilic reactions. According to Koopmann approximation, molecular softness (S) was computed by HOMO/LUMO energies [*i.e.*, $S = 1/(E_{LUMO} - E_{HOMO})$], as derived by semiempiric calculations by using MOPAC2009 (Keywords: "PM6," "PRECISE," "GEO-OK," and "MULLIK"). When more adducts were possible, the potential regioselectivity of monitored additions was investigated by calculating local reactivity descriptors, as expressed by condensed atom Fukui indices (3).

Results

HNE-induced carbonylation of Hb

The first step of this work was to evaluate the ability of EDA to inhibit protein carbonylation, by using Hb as a model protein covalently modified by HNE, the highly reactive α,β-unsaturated aldehyde generated by lipid peroxidation. To do this, high-resolution mass spectrometry was initially used to study the stoichiometry of the Hb-HNE reaction, and to identify the target nucleophilic sites for HNE adduction on the protein, never reported in the literature. Figure 1a shows the ESI-MS spectrum of human Hb recorded at a resolution of 100,000, characterized by several multicharged ions relative to the beta (Hbβ) and alpha (Hbα) chain (see the deconvoluted spectrum in Fig. 1b). When Hb was incubated in the presence of HNE at a molar ratio 1:1 for 120 min at 37°C (Fig. 2a), no detectable adducts of both α and β chains were observed. By increasing the HNE concentration (Hb/HNE molar ratio, 1:5), a very detectable HNE adduct of the β chain was observed at 16,022.41 Da, shifted by + 156 Da with respect to the native form (15,866.26 Da), and attributed to the HNE Michael adduct (Fig. 2b). By further increasing the HNE concentration (1:10 molar ratio; Fig. 2c), the relative abundance of the adduct increased in a dose-dependent manner, to reach a relative abundance greater than 10%. No adducts on the α chain were observed at all the HNE concentrations tested (Fig. 2).

In a second set of experiments, the incubation time was extended to 240 min. In these conditions, HNE (Hb/HNE molar ratio, 1:10) induced a weak, but significant HNE-

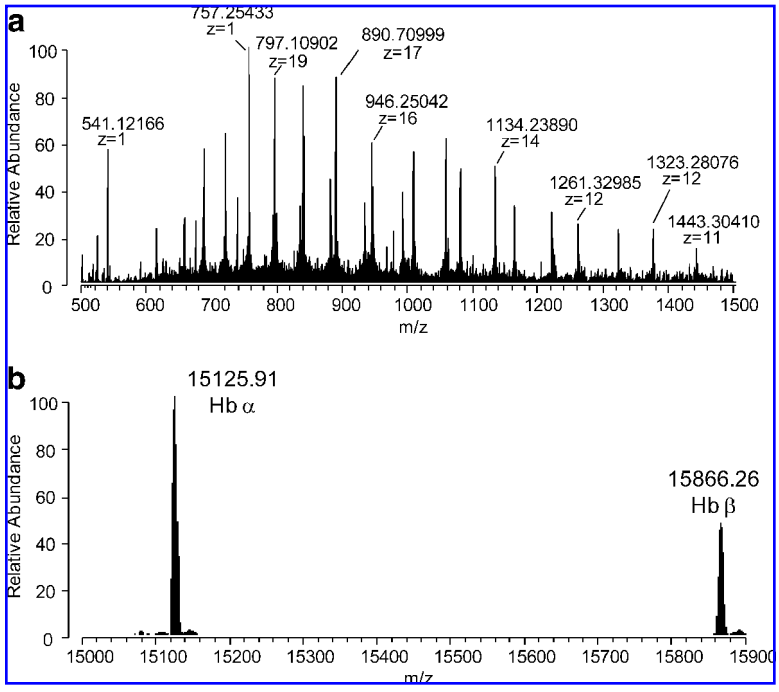

FIG. 1. Direct-infusion ESI-MS analysis of human Hb. (**a**) MS spectrum of Hb recorded in positive ion mode at a resolution of 100,000 (Orbitrap as analyzer); (**b**) deconvoluted spectrum showing peaks relative to α (15,125.91 Da) and β (15,866.26) Hb chains.

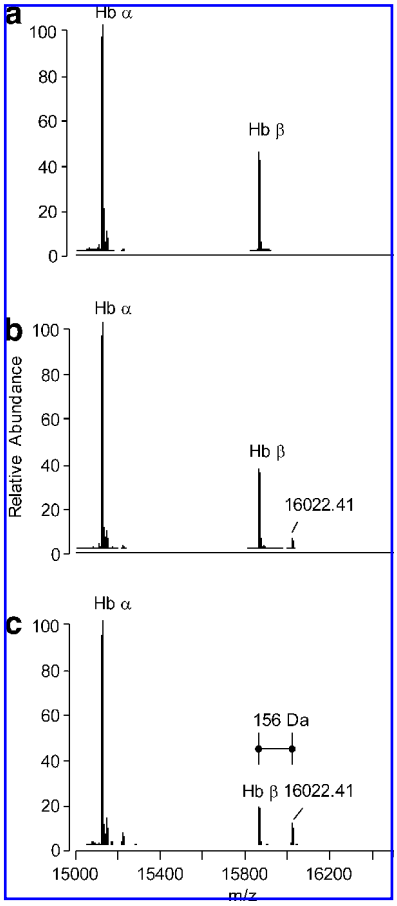

FIG. 2. HNE-induced carbonylation of Hb. Deconvoluted ESI-MS spectra of Hb incubated with HNE for 120 min at different Hb/HNE molar ratios: (**a**) 1:1; (**b**) 1:5; (**c**) 1:10. The HNE Michael adduct of the β chain is observed at 16,022.41 Da, shifted by + 156 Da with respect to the native form (15,866.26 Da).

covalent modification of the α chain, which was detected at 15,282.08, consistent with a shift of 156 Da compared with the native α chain. The abundance of the Michael adduct on the β chain significantly increased with respect to the native chain, and, in addition, a double HNE Michael adduct appeared at 16,177.53 Da (Fig. 3).

The adducted amino acids were then characterized with LC-ESI-MS analysis of trypsin-digested Hb, previously incubated for 240 min with HNE (Hb/HNE, 1:10 molar ratio) and then reduced by $NaBH_4$. HNE is well known to react through a Michael adduction with the nucleophilic sites of His, Lys, and Cys, as well as to form a Schiff base with the ε-amino group of lysine (2). Based on these well-known reaction mechanisms, the covalent modifications of the nucleophilic sites (His, Lys, Cys) with HNE were predicted and, for each adduct, the monoisotopic mass shift of the corresponding reduced form was calculated and used as a variable modification in the Sequest search. By using this approach, several HNE Michael adducts were identified on both Hb chains. Table 1 summarizes the covalently modified sites involving the Michael adduct formation on His, Lys, and Cys residues, and the Schiff base on the Lys residue. Besides a qualitative pattern, we also were interested in comparing the chemical reactivity of the target amino acids toward HNE, to identify the most reactive and nucleophilic sites. To do this, the chromatographic peak of each modified peptide was reconstituted by selecting the most intense multicharged ion as filter, and the peak areas were calculated and compared with those of the corresponding unmodified peptides. The results reported in Table 1 indicate Cysβ93 as the most reactive site, because the peptide containing the HNE modification accounts for more than 40% of the Cysβ93-containing peptides. Figure 4 shows the reconstituted LC-ESI-MS chromatogram by using as filter ions the m/z 739.85082 and 790.40543 relative to the $[M + 2H]^{2+}$ of the native and adducted peptides, respectively.

Molecular-modeling studies were then performed with a view to explaining the different abundance of the monitored adducts. As compiled in Table 2, three parameters were considered in this computational analysis: (a) the accessibility of each considered residue, as defined by its SAS value; (b) the predicted ionization constants, as computed by pKaTool (18); and (c) the interaction energy, as derived by docking simulation for the closest pose. Table 2 clearly indicates that all monitored residues are significantly accessible, even if the His residues are, on average, more exposed than the Lys and Cys residues. Again, Table 2 shows that all residues possess a pK_a constant quite similar to that of the corresponding free residue, meaning that the protein microenvironment does not vastly affect the ionization state of such residues. This result can justify the marked abundance of the Cysβ93 adduct because, at physiologic pH, a significant fraction of reactive thiolate anion is found, as well as the modest abundance of Lys adducts, because, at physiologic pH, the unreactive protonated forms are largely predominant. Additionally, the docking scores, as computed for the closest pose of each residue, are in line with the adduct abundances, showing that the complex with HNE close to Cysβ93 yields the vastly lowest interaction energy. Figure 5 depicts such minimized complex unveiling that HNE is accommodated in a polar crevice at the interface between the two subunits, where it can stabilize some significant contacts. Specifically, the aldehydic carbonyl group forms an H-bond with Hisβ97, whereas the C4 hydroxyl function stabilizes a network of H-bonds that involves Lysα40, Aspβ94, and Hisβ146. Modeling analyses also can explain why Cysβ93 is the only Cys residue yielding adducts with HNE. The other two Cys residues (Cysβ104 and Cysβ112) are markedly less acid ($pK_a > 10$) and totally buried, as confirmed by the fact that no docking pose exists where HNE is reasonably close to such cysteines.

Edaravone inhibits Hb carbonylation

When EDA was co-incubated for 120 min in the presence of fixed concentrations of Hb and HNE (1:10 molar ratio), it was found dose-dependently to inhibit Hb carbonylation (Fig. 6). The protective effect started at 40 μM (Fig. 6b), a concentration able to reduce by $24 \pm 4\%$ the Hb-HNE adduct formation, taking as 100% formation that found in samples incubated in the absence of EDA (Fig. 6a). The protective effect dose-dependently increased, reaching a $92 \pm 2\%$ inhibition at 200 μM (Fig. 6c). The signal for the Hb-HNE adduct was undetectable in samples incubated with 400 μM EDA (100% inhibition) (Fig. 6d).

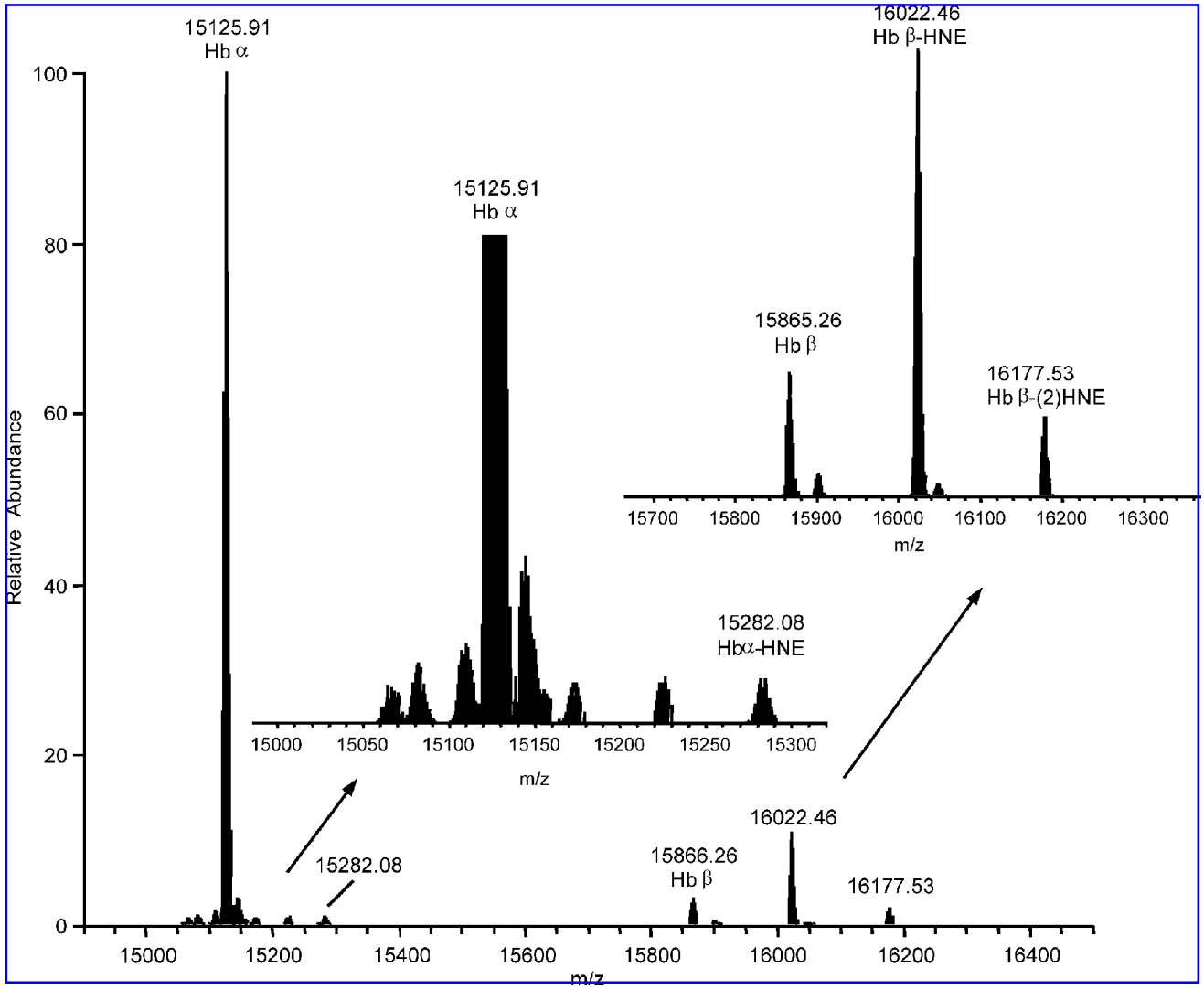

FIG. 3. HNE-induced carbonylation of Hb. Deconvoluted ESI-MS spectra of Hb incubated with HNE for 240 min at 1:10 Hb/HNE molar ratio.

Table 1. Identified HNE-Adducted Peptides on Hb

Peptide sequence	*Adduction site*	*Adduct type*	*[M+H]$^+$*	*Delta (ppm)**	*P(pro)†*	*Peak area (%)‡*
Hbα						
VGAHAGEYGAEALER	H20	MA	1687.86497	−0.7	4.54E-13	3.43
TYFPHFDLSHGSAQVK	H45	MA	1992.02253	−1.5	1.17E-12	1.96
TYFPHFDLSHGSAQVK	H50	MA	1992.02253	−0.4	8.99E-05	1.96
Hbβ						
VHLTPEEK	H2	MA	1110.64049	−0.3	2.18E-06	4.5
LHVDPENFR	H97	MA	1284.69465	−1.3	5.78E-08	3.7
VVAGVANALAHK	H143	MA	1307.80454	−0.9	2.83E-09	4.4
GTFATLSELHCDK	C93	MA	1579.80361	−0.4	2.38E-08	41.03
VLGAFSDGLAHLDNLK	H77	MA	1828.02147	−0.6	2.50E-11	0.84
VVAGVANALAHKYH	K144	SB	1589.91622	−0.5	6.5E-12	0.31

Hb was digested with trypsin following incubation with HNE (Hb:HNE 1:10 molar ratio) for 240 min at 37°C.
MA, Michael adduct; SB, Schiff base.
*Delta (ppm) with respect to the calculated [M+H]$^+$ values.
†Displays the probability of finding a match as good as or better than the observed match by chance.
‡Peak area (%) of the adducted peptides with respect to the peak area of the corresponding unmodified peptides.

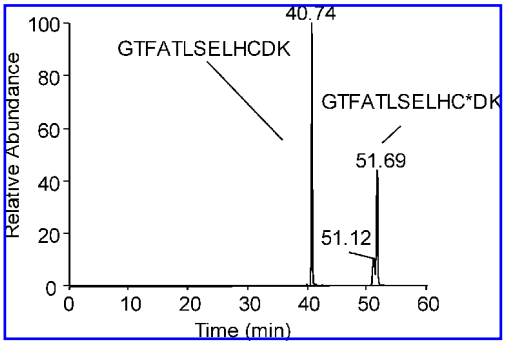

FIG. 4. Cys93 on Hb β chain is the most reactive site toward HNE adduction. Reactivity of each adducted amino acid residue was determined by comparing the peak area of the modified peptide with that of the corresponding unmodified peptide. The figure shows the reconstituted LC-ESI-MS chromatogram of native and adducted Cys93-containing peptides, by using as filter ions the m/z 739.85082 and 790.40543 relative to the $[M+2H]^{2+}$ of the native and adducted peptides, respectively.

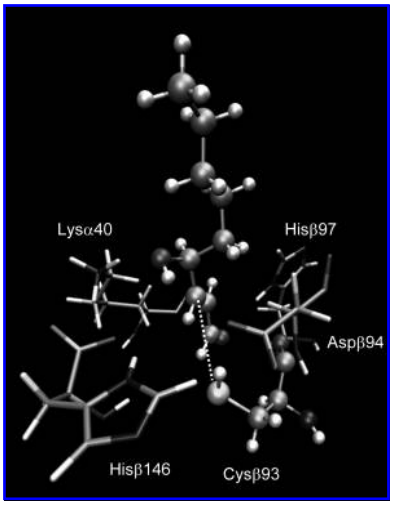

FIG. 5. Main interactions stabilizing the best pose of HNE close to Cys93, as derived with docking simulations. Notice that HNE is conveniently inserted in a polar crevice where carbonyl and C-4 hydroxyl groups can realize relevant polar contacts.

RCS-scavenging activity (reactivity)

To gain a deeper insight into the mechanism of protein-carbonylation inhibition, the direct HNE-scavenging ability of EDA was then evaluated, by measuring the consumption of the target aldehyde with HPLC analysis. Table 3 includes the scavenging activities of EDA toward HNE, and the results are compared with those of selected reference compounds (PYR, L-CAR, and HY), which are well-known RCS-sequestering agents, as already reported (28). EDA was found to be the most reactive compound toward HNE, leading to an almost total disappearance of the aldehyde after 180 min of incubation. The scavenging activity of EDA was then extended to other RCS (ACR and GO), and also with these target aldehydes, the EDA potency was far greater than that of the other sequestering agents.

Table 2. Reactivity of the Adduction Sites as Analyzed by Modeling Studies

Adduction site	*Peak area (%)**	*pK residue*	*Solvent accessibility*	*Docking score*
Hbα				
H20	3.43	5.9	74.8	−28.5
H45	1.96	5.5	57.4	−52.1
H50	1.96	5.9	178.7	−41.8
Hbβ				
H2	4.5	6.0	180.5	−49.2
H97	3.7	5.1	67.6	−51.8
H143	4.4	5.4	76.7	−47.5
K144	4.4	9.7	82.6	−51.7
C93	41.03	8.5	28.7	−65.3
K82	0.84	9.1	101.3	−45.9
H77	0.84	5.2	78.1	−49.2

Reactivity was parameterized in terms of ionization state (expressed by predicted pK_3 values), solvent accessibility (as computed by SAS surface, Å^3), and interaction capacities (evaluated by docking score for the closest pose, Kcal/mol).

*Peak area (%) of the adducted peptides with respect to the peak area of the corresponding unmodified peptides.

The entrapping capacity of EDA was further confirmed by identifying the RCS-EDA reaction products with direct-infusion MS analysis in full-scan mode. As a preamble, it is worth mentioning that several theoretic and experimental studies showed that the most electrophilic center in an α,β-unsaturated aldehyde is the C3 atom (13), meaning that when it reacts with a carbonion (as in the case of edaravone), the Michael addition is largely prevalent on the mixed aldolic condensation. Hence, only the reaction mechanisms starting with a Michael addition were monitored here. Figure 7a shows the MS spectrum of EDA, characterized by a base peak at m/z 175.2 relative to the $[M+H]^+$ ion. The MS spectrum recorded after 180-min incubation was superimposable, to indicate the stability of EDA in the experimental conditions used (data not shown). When EDA was incubated for 180 min in the presence of HNE, the MS spectrum contained, besides the $[M+H]^+$ ion of unreacted EDA, an abundant ion at m/z 661.2 (base peak), accompanied by the corresponding $[M+Na]^+$ adduct at m/z 683.2, and a minor reaction product ion at m/z 487.2 (Fig. 7b). The MWs of the adducts were then determined by using Orbitrap as mass analyzer, and the empiric formula was calculated on the basis of the exact masses by using the Xcalibur Software. The results are summarized in Table 4, and the proposed reaction mechanism of EDA with HNE is schematically summarized in Fig. 8. The reaction starts with the formation of a Michael adduct between the C3 of HNE and the acid methylene group in α to carbonyl to give 1b, which then reacts through a mixed aldolic condensation with a second EDA molecule to form, after dehydration, the 2b derivative. Such a compound, being characterized by an α,β-unsaturated moiety, reacts with a third EDA molecule to give the final product, 3b.

When EDA was incubated with ACR for 180 min, besides the $[M+H]^+$ ion relative to the unreacted EDA, several other ions appeared, among which were those at m/z 617.2 (base peak), m/z 561.14 (35%), 387.1 (30%), and 231.2 (34%) (Fig. 7c). The accurate masses of the reaction products were then

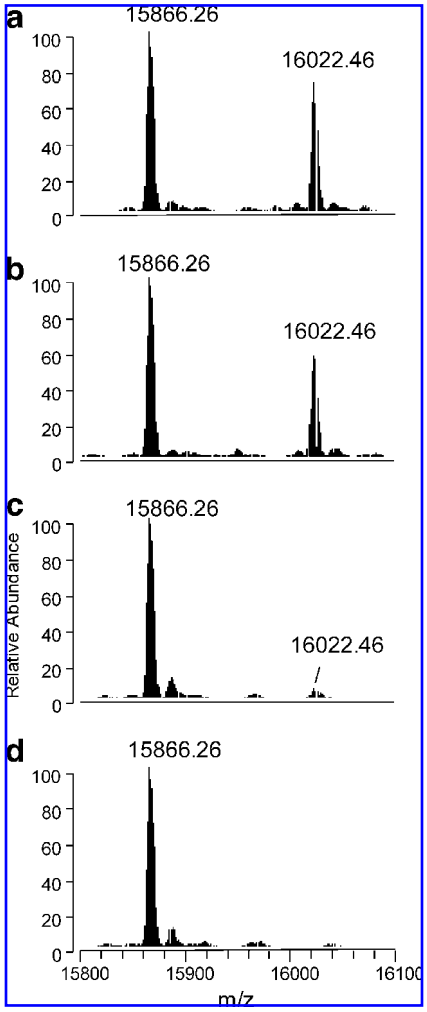

FIG. 6. EDA dose-dependently inhibits HNE-induced carbonylation of Hb. The dose-dependent effect of EDA on Hb carbonylation was studied by co-incubating Hb for 120 min with 200 μM HNE and different EDA doses (40, 200, and 400 μM). The figure shows the mass spectra of Hb incubated in the absence (**a**) and in the presence of increasing EDA concentrations: 40 (**b**), 200 (**c**), and 400 μM (**d**).

determined by using Orbitrap as a mass analyzer (resolution, 100,000) (Table 4). The proposed reaction mechanism of EDA with ACR is schematically summarized in Fig. 9. The first step involves formation of a Michael adduct, forming compound 1d. Compound 1d further reacts with a second EDA molecule through an aldolic condensation and dehydration, giving 2d. This intermediate, being characterized by an α,β-unsaturated moiety, reacts with another EDA molecule, yielding compound 3d, which in turn reacts with ACR to form two 4d derivatives, which differ in adduct position. Again, 4d isomers can yield a mixed aldolic condensation with a fourth EDA molecule to form 5d positional isomers.

The molecular softness values for monitored adducts (Table 4) explain the particular reactivity of EDA toward α,β-unsaturated aldehydes. In particular, the molecular softness values allow two relevant considerations: (a) the adducts being characterized by α,β-unsaturated moieties are markedly more reactive than are those having an acid methylene, confirming that the Michael addition is largely preferred, compared with aldolic condensation; and (b) all considered adducts show a molecular softness similar to or greater than that of EDA. This is understandable, considering that all adducts conserve either an α,β-unsaturated moiety or an acid methylene, and suggests that EDA can react with α,β-unsaturated aldehydes, acting as a polymerizing agent and forming adducts characterized by very high molecular weights. It should be noted that local reactivity descriptors (as expressed by condensed atom Fukui indices) were computed when more adduct positions were possible to unveil whether the examined adduction could have a certain degree of regioselectivity. Nonetheless, the very similar Fukui indices for 4d and for 5d derivatives suggest that such positional isomers are almost equally probable.

Pyridoxal-scavenging activity (selectivity)

The ability of EDA, compared with that of the reference compounds, to react exclusively with cytotoxic RCS (no reaction with physiologically relevant aldehydes), was determined by using pyridoxal as target aldehyde. HPLC analyses indicated that EDA and HY, unlike L-CAR, induce a significant depletion of pyridoxal, after 180-min incubation (Table 2). The lack of selectivity of EDA was further confirmed with MS analysis of the incubation mixtures. The ESI-MS spectra are indeed characterized by the reduction of the $[M+H]^+$ signal relative to the scavenger at m/z 175.2, accompanied by the formation of the reaction products at m/z 498.15 and 324.2 (Fig. 7d). Figure 10 summarizes the proposed EDA-PYAL reaction mechanism, involving as a first step a mixed aldolic condensation to yield 1f. Dehydration of this intermediate gives 2f, which, bearing an α,β-unsaturated moiety, reacts with a second EDA molecule to give 3f.

Table 3. Reactivity and Selectivity of EDA and Selected Reference Compounds

	Reactivity			*Selectivity*
QUENCHER	HNE (%)	ACR (%)	GO (%)	PYAL (%)
Edaravone	1.08 ± 0.04	0.4 ± 0.09	3.97 ± 0.25	2.21 ± 0.51
Pyridoxamine	87.37 ± 2.06	25.52 ± 1.34	89.45 ± 1.74	N.D.
Hydralazine	7.66 ± 0.13	5.49 ± 1.11	35.23 ± 3.29	19.84 ± 4.21
L-Carnosine	64.99 ± 1.50	27.97 ± 1.99	97.25 ± 2.11	96.90 ± 2.54

Results are reported as percentage of RCS and PYAL remaining with respect to a blank incubated in the absence of the tested compound. Values are the mean $\pm$ S.D. of 4 determinations.

N.D., not determined.

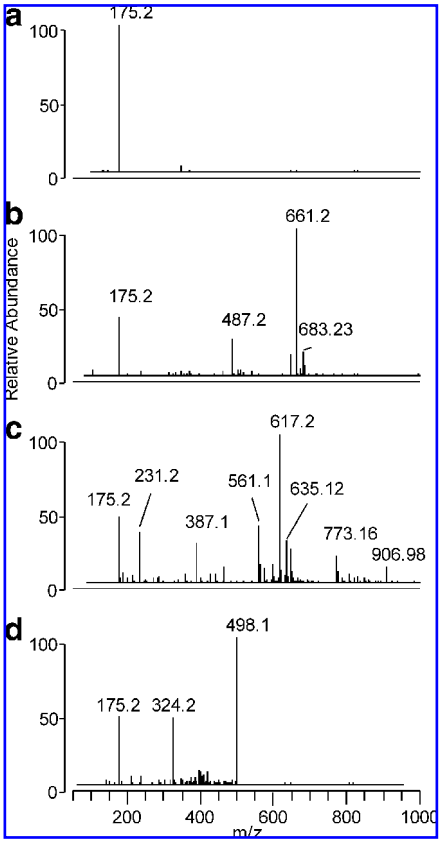

FIG. 7. RCS-EDA reaction products: identification with direct-infusion ESI-MS analysis. Mass spectra (triple-quadrupole mass spectrometer) were acquired in full-scan mode. EDA (0.5 m*M*) was incubated for 180 min in 1 m*M* phosphate buffer (pH 7.4) in the absence (**a**) and in the presence of an equimolar concentration of HNE (**b**), ACR (**c**), and PYAL (**d**).

Discussion

In view of the growing need to find new molecules sharing both antioxidant and carbonyl scavenger properties to restrain lipid-derived oxidative/carbonyl stress associated with a variety of pathologic conditions, we focus our study on edaravone, a compound already known as a potent radical scavenger, whose carbonyl-sequestering ability, however, has been poorly investigated. The only report available limited the evaluation to the trapping ability toward glyoxal and methylglyoxal, dialdehydes that are precursors of EAGLEs and AGEs, respectively (14). Edaravone has been shown to be effective in a variety of oxidative stress–related diseases owing to its antioxidant potency. Because intervention strategies based on a direct radical-scavenging (antioxidant) approach, which provides a first line of defense against free radicals, such as vitamins E and C, failed to show beneficial effects in ROS-dependent diseases (2), we thought that edaravone intervention as a free radical scavenger could be questionable, and not solely accountable for the beneficial effects demonstrated in both pharmacologic and clinical studies (29). This consideration, associated with the emerging role of RCS derived by ROS-induced decomposition of polyunsaturated fatty acids as pathogenic factors, and to the concept of carbonylation damage as a new drug target (1, 2, 17), prompted us to investigate in detail the RCS-entrapping ability and potency of EDA.

With Hb as a protein model, the results of the first part of this study demonstrate that EDA inhibits Hb carbonylation induced by HNE through a direct trapping mechanism. The covalent modification of Hb by HNE, never reported, involves Cys93 of the β chain, as demonstrated by a combined high-resolution mass-spectrometric and computational approach. Our results are quite different from those reported by Yocum *et al*. (31), who studied the covalent modifications of Hb after incubation with 4-oxo-nonenal as a lipid-derived target aldehyde, by using MALDI-TOF/MS analysis of the intact protein and a combination of LC-ESI-MS/MS and MALDI-TOF/MS/MS analysis of the tryptic peptides. Although incubation conditions were different from those reported in this study, they found covalent modifications on both Hb chains and identified Hys20 (α chain) and His63 (β chain) as the target nucleophilic sites for 4-oxo-nonenal adduction, a finding supported by molecular modeling, indicating these two residues as the most solvent accessible in intact Hb.

Nonetheless, it should be noted that our modeling analyses confirmed the marked exposition of His20, but unveiled that

Table 4. Accurate Mass of EDA Reaction Products with HNE, ACR, and PYAL Determined by High Resolution Mass Spectrometry (Orbitrap)

	m/z	*Formula [M+H]$^+$*	*Accuracy (ppm)*	*Molecular softness (S, au)*
HNE adduct				
2b	487.27104	$C_{29}H_{35}N_4O_3$	1.4	0.133
3b	661.35070	$C_{39}H_{45}N_6O_4$	1.5	0.119
ACR adduct				
1d	231.11295	$C_{13}H_{15}N_2O_2$	0.631	0.133
2d	387.18209	$C_{23}H_{23}N_4O_2$	1.4	0.141
3d	561.2614	$C_{33}H_{33}N_6O_3$	0.9	0.120
4d	617.28687	$C_{36}H_{37}N_6O_4$	−0.34	0.123
PYR adduct				
2f	324.13481	$C_{18}H_{18}N_3O_3$	1.7	0.136
3f	498.21412	$C_{28}H_{27}N_5O_4$	1.1	0.125

Elemental composition of each compound was calculated by Elemental composition feature included in Xcalibur Qual Browser 2.0. Molecular softness for the monitored adducts was computed by semiempirical calculations. Notice that the molecular softness of EDA is equal to 0.116 au.

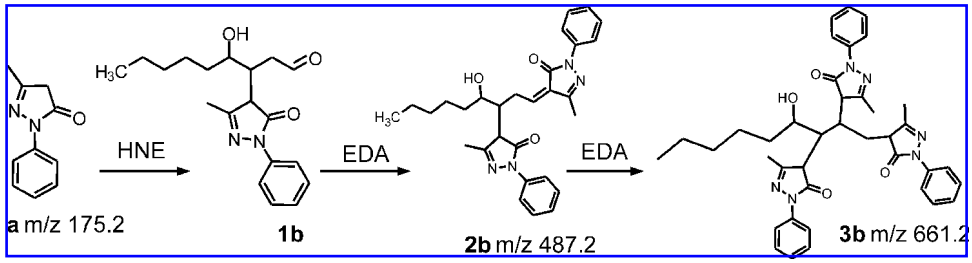

FIG. 8. Proposed reaction mechanism of EDA with HNE. The m/z values indicate protonated molecules.

His63 is quite inaccessible (SAS = 7.2 Å^2), thus explaining why the adduct on His63 was not detected in the present study.

Our findings indicate that Cysβ93 Hb modifications can be used not only as a reliable *in vitro* model to screen rapidly the ability of newly developed RCS sequestering agents to inhibit protein carbonylation, but also as a potential biomarker *in vivo* of lipid-derived macromolecule damage. The ability of EDA to prevent Hb modification by HNE, the prototype of cytotoxic α,β-unsaturated aldehydes derived from lipid peroxidation, served as the first convincing evidence to undertake a detailed investigation of the RCS-entrapping capacity of the compound, providing new information on its reactivity (a ranking of potency within a series of well-known RCS-sequestering agents has been established), its ability to spare physiologically relevant aldehydes, such as pyridoxal (selectivity), and on the mechanisms involved in EDA interaction with both α,β-unsaturated aldehydes and pyridoxal.

The results of this part of the study confirm that EDA traps glyoxal and demonstrate for the first time that the compound, unlike L-carnosine, but like hydralazine, traps both highly cytotoxic α,β-unsaturated aldehydes, precursors of ALEs, HNE, and acrolein, but also pyridoxal, an effect already observed, but not mechanistically explained by Izuhara *et al.* (14). The combined mass spectrometric and computational approach allowed us to explain the EDA reactivity and to furnish a deeper insight into the mechanism of interaction with both RCS and pyridoxal, also taking into account the mechanism of antioxidant intervention. The antioxidant properties of edaravone are interpretable, considering its acidity (pK_a = 6.90) and the capacity of its anionic form to scavenge

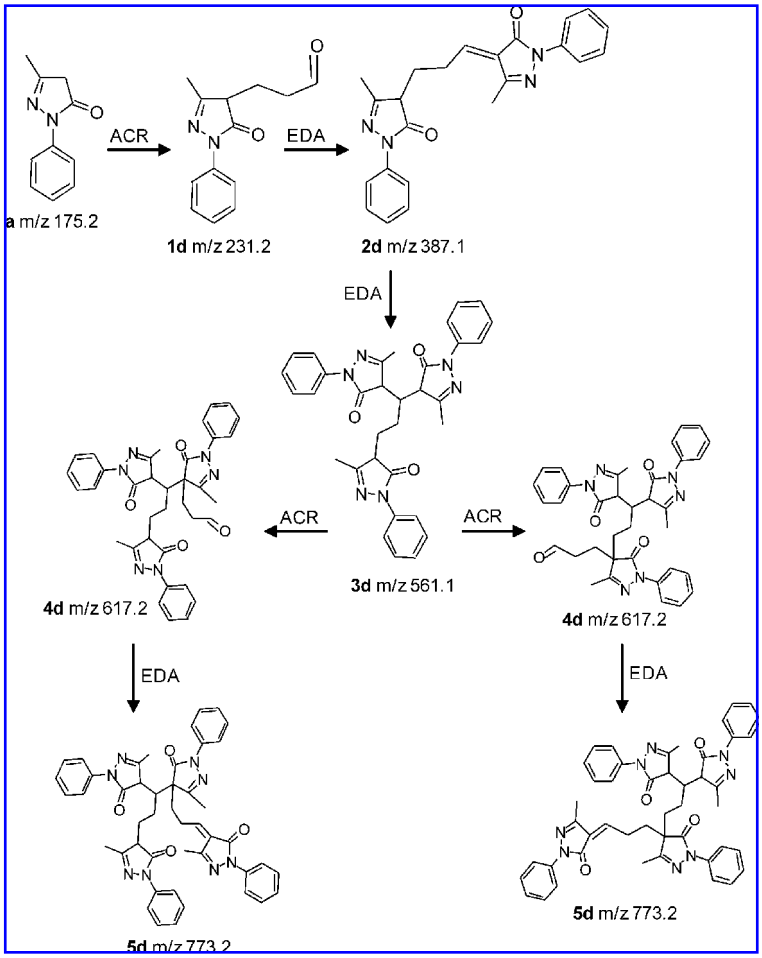

FIG. 9. Proposed reaction mechanism of EDA with ACR. The m/z values indicate protonated molecules.

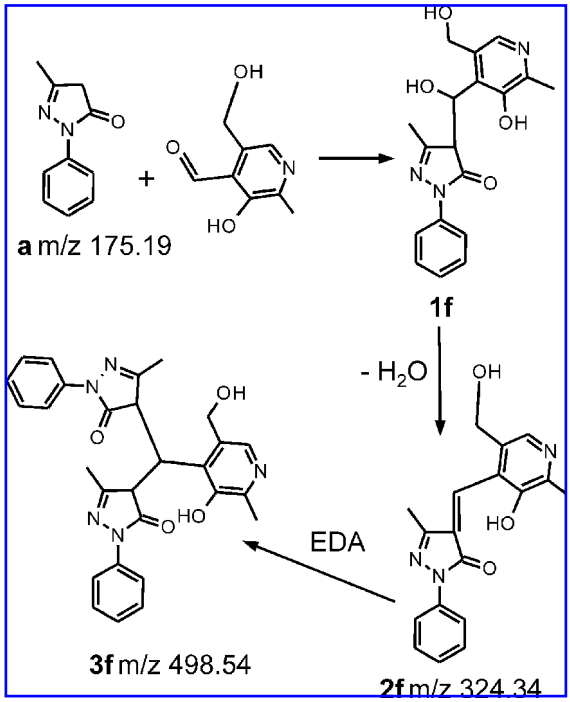

FIG. 10. Proposed reaction mechanism of EDA with PYAL. The m/z values indicate protonated molecules.

free radicals, yielding a nonreactive anion plus an edaravone radical, which is transformed into 4,5-dione *via* edaravone peroxyl radical with the reaction of molecular oxygen, followed by hydrolysis to afford 2-oxo-3-(phenyl hydrazono)-butanoic acid (29). Such a mechanism can occur in both polar and hydrophobic media with small differences, and indeed, edaravone is thought to act near or probably on the cell membranes (13). Similarly, the capacity of edaravone to scavenge reactive carbonyl species is understandable, considering that the acid methylene group in α to carbonyl can yield aldolic condensation with whichever carbonyl compounds are present. This means that EDA is an efficient, but not a specific scavenger of carbonyl species and explains its ability to trap pyridoxal. This lack of selectivity obviously precludes its long-term administration in humans, unless adequate vitamin B_6 supplementation is provided.

The high reactivity with α,β-unsaturated aldehydes (EDA is far more potent than the other structurally unrelated RCS scavengers considered) and the ability to inhibit protein carbonylation shed light on a new mechanism by which the compound can exert its efficacy *in vivo* and open new perspectives to start a rational design of EDA analogues, maintaining the same RCS-scavenging potency, but characterized by an increased selectivity.

Acknowledgments

This research was supported by funds from University of Milan (PUR 2007, 2008) and from MIUR (PRIN 2007).

Author Disclosure Statement

No competing financial interests exist.

References

1. Aldini G, Dalle-Donne I, Colombo R, Maffei Facino R, Milzani A, and Carini M. Lipoxidation-derived reactive carbonyl species as potential drug targets in preventing protein carbonylation and related cellular dysfunction. *Chem Med Chem* 1: 1045–1058, 2006.
2. Aldini G, Dalle-Donne I, Facino RM, Milzani A, and Carini M. Intervention strategies to inhibit protein carbonylation by lipoxidation-derived reactive carbonyls. *Med Res Rev* 27: 817–168, 2007.
3. Balawender R and Komorowski L. Atomic Fukui function indices and local softness ab initio. *J Chem Phys* 109: 5203–5211, 1998.
4. Butterfield DA and Castegna A. Proteomics for the identification of specifically oxidized proteins in brain: technology and application to the study of neurodegenerative disorders *Amino Acids* 25: 419–425, 2003.
5. Butterfield DA, Sultana R, and Poon HF. Redox proteomics: a new approach to investigate oxidative stress in Alzheimer's disease. In: *Redox Proteomics: From Protein Modifications to Cellular Dysfunction and Disease,* edited by Dalle-Donne I, Scaloni A, and Butterfield DA. Hoboken: Wiley, 2006, pp. 563–603.
6. Carini M, Aldini G, and Maffei Facino R. Mass spectrometry for detection of 4-hydroxy-trans-2-nonenal (HNE) adducts with peptides and proteins. *Mass Spectrom Rev* 23: 281–305, 2004.
7. Crabb JW, O'Neil J, Miyagi M, West K, and Hoff HF. Hydroxynonenal inactivates cathepsin B by forming Michael adducts with active site residues. *Protein Sci* 11: 831–840, 2002.
8. Dalle-Donne I, Rossi R, Giustarini D, Milzani A, and Colombo R. Protein carbonyl groups as biomarkers of oxidative stress. *Clin Chim Acta* 329: 23–38, 2003.
9. Dalle-Donne I, Scaloni A, Giustarini D, Cavarra E, Tell G, Lungarella G, Colombo R, Rossi R, and Milzani A. Proteins as biomarkers of oxidative/nitrosative stress in diseases: the contribution of redox proteomics. *Mass Spectrom Rev* 24: 55–99, 2005.
10. Dalle-Donne I, Aldini G, Carini M, Colombo R, Rossi R, and Milzani A. Protein carbonylation, cellular dysfunction, and disease progression. *J Cell Mol Med* 10: 389–406, 2006.
11. Domingo LR, Benchoukb W, and Mekellecheb SM. Understanding the role of the Lewis acid catalyst on the 1,3-dipolar cycloaddition of *N*-benzylideneaniline *N*-oxide with acrolein: a DFT study. *Tetrahedron* 63: 4464–4471, 2007.
12. Fenaille F, Guy PA, and Tabet JC. Study of protein modification by 4-hydroxy-2-nonenal and other short-chain aldehydes analyzed by electrospray ionization tandem mass spectrometry. *J Am Soc Mass Spectrom* 14: 215–226, 2003.
13. Higashi Y. Edaravone for the treatment of acute cerebral infarction: role of endothelium-derived nitric oxide and oxidative stress. *Expert Opin Pharmacother* 10: 323–331, 2009.
14. Izuhara Y, Nangaku M, Takizawa S, Takahashi S, Shao J, Oishi H, Kobayashi H, van Ypersele de Strihou C, and Miyata T. A novel class of advanced glycation inhibitors ameliorates renal and cardiovascular damage in experimental rat models. *Nephrol Dial Transplant* 23: 497–509, 2008.
15. LoPachin RM, Barber DS, and Gavin T. Synaptosomal toxicity and nucleophilic targets of 4-hydroxy-2-nonenal. *Toxicol Sci* 104: 235–249, 2008.
16. Miyata T, van Ypersele de Strihou C, Ueda Y, Ichimori K, Inagi R, Onogi H, Ishikawa N, Nangaku M, and Kurokawa

K. Angiotensin II receptor antagonists and angiotensin-converting enzyme inhibitors lower in vitro the formation of advanced glycation end products: biochemical mechanisms. *J Am Soc Nephrol* 13: 2478–2487, 2002.
17. Negre-Salvayre A, Coatrieux C, Ingueneau C, and Salvayre R. Advanced lipid peroxidation end products in oxidative damage to proteins: potential role in diseases and therapeutic prospects for the inhibitors. *Br J Pharmacol* 153: 6–20, 2008.
18. Nielsen JE. Analysing the pH-dependent properties of proteins using pKa calculations. *J Mol Graph Model* 25: 691–699, 2007.
19. Nyström T. Role of oxidative carbonylation in protein quality control and senescence. *EMBO J* 24: 1311–1317, 2005.
20. O'Brien PJ, Siraki AG, and Shangari N. Aldehyde sources, metabolism, molecular toxicity mechanisms, and possible effects on human health. *Crit Rev Toxicol* 35: 609–662, 2005.
21. Olsen JV, de Godoy LM, Li G, Macek B, Mortensen P, Pesch R, Makarov A, Lange O, Horning S, and Mann M. Parts per million mass accuracy on an Orbitrap mass spectrometer via lock mass injection into a C-trap. *Mol Cell Proteomics* 12: 2010–2021, 2005.
22. Pedretti A, Villa L, and Vistoli G. Modeling of binding modes and inhibition mechanism of some natural ligands of farnesyl transferase using molecular docking. *J Med Chem* 45: 1460–1465, 2002.
23. Pennathur S and Heinecke JW. Mechanisms for oxidative stress in diabetic cardiovascular disease. *Antioxid Redox Signal* 9: 955–969, 2007.
24. Poli G, Schaur RJ, Siems WG, and Leonarduzzi G. 4-Hydroxynonenal: a membrane lipid oxidation product of medicinal interest. *Med Res Rev* 28: 569–631, 2008.
25. Rees MS, van Kuijk FJGM, Siakotos AN, and Mundy BP. Improved synthesis of various isotope labelled 4-hydroxyalkenals and peroxidation intermediates. *Synth Commun* 25: 3225–3228, 1995.
26. Kind T and Fiehn O. Seven golden rules for heuristic filtering of molecular formulas obtained by accurate mass spectrometry. *BMC Bioinformatics* 8: 105–121, 2007.
27. Uchida K. Role of reactive aldehyde in cardiovascular diseases. *Free Radic Biol Med* 28: 1685–1696, 2000.
28. Vistoli G, Orioli M, Pedretti A, Regazzoni L, Canevotti R, Negrisoli G, Carini M, and Aldini G. Design, synthesis, and evaluation of carnosine derivatives as selective and efficient sequestering agents of cytotoxic reactive carbonyl species. *Chem Med Chem* 4: 967–975, 2009
29. Watanabe T, Tahara M, and Todo S. The novel antioxidant edaravone: from bench to bedside. *Cardiovasc Ther* 26: 101–114, 2008.
30. Xi H, Akishita M, Nagai K, Yu W, Hasegawa H, Eto M, Kozaki K, and Toba K. Potent free radical scavenger, edaravone, suppresses oxidative stress-induced endothelial damage and early atherosclerosis. *Atherosclerosis* 191: 281–289, 2007.
31. Yocum AK, Yergey AL, and Blair IA. Novel lipid hydroperoxide-derived hemoglobin histidine adducts as biomarkers of oxidative stress. *J Mass Spectrom* 40: 754–764, 2005.
32. Zhang N, Komine-Kobayashi M, Tanaka R, Liu M, Mizuno Y, and Urabe T. Edaravone reduces early accumulation of oxidative products and sequential inflammatory responses after transient focal ischemia in mice brain. *Stroke* 3: 2220–2225, 2005.

Address correspondence to:
Marina Carini
Dipartimento di Scienze Farmaceutiche "Pietro Pratesi"
Università degli Studi di Milano
Via L. Mangiagalli 25
20133 Milan, Italy

E-mail: marina.carini@unimi.it

Date of first submission to ARS Central, August 7, 2009; date of acceptance August 15, 2009.

Abbreviations Used

ACR = acrolein
AGEs = advanced glycation end products
ALEs = advanced lipoxidation end products
EAGLEs = either advanced glycation or lipoxidation end products
EDA = edaravone
GO = glyoxal
GSH = glutathione
GSSG = glutathione disulfide
Hb = hemoglobin
HNE = 4-hydroxy-*trans*-2-nonenal
HY = hydralazine
LC-ESI-MS/MS = liquid chromatography-electrospray ionization tandem mass spectrometry
MALDI-TOF MS = matrix-assisted laser desorption ionization time-of-flight mass spectrometry
nano ESI-LC-MS/MS = nanoscale liquid chromatography-electrospray ionization tandem mass spectrometry
PYAL = pyridoxal
PYR = pyridoxamine.
RCS = reactive carbonyl species
ROS = reactive oxygen species

This article has been cited by:

1. Graziano Colombo, Isabella Dalle-Donne, Marica Orioli, Daniela Giustarini, Ranieri Rossi, Marco Clerici, Luca Regazzoni, Giancarlo Aldini, Aldo Milzani, D. Allan Butterfield, Nicoletta Gagliano. 2012. Oxidative damage in human gingival fibroblasts exposed to cigarette smoke. *Free Radical Biology and Medicine* **52**:9, 1584-1596. [CrossRef]
2. Irfan Rahman, Vuokko L Kinnula. 2012. Strategies to decrease ongoing oxidant burden in chronic obstructive pulmonary disease. *Expert Review of Clinical Pharmacology* **5**:3, 293-309. [CrossRef]
3. Irfan Rahman, William MacNee. 2012. Antioxidant pharmacological therapies for COPD. *Current Opinion in Pharmacology* . [CrossRef]
4. Irfan Rahman. 2011. Pharmacological Antioxidant Strategies As Therapeutic Interventions For Copd. *Biochimica et Biophysica Acta (BBA) - Molecular Basis of Disease* . [CrossRef]
5. Navin Rauniyar, Laszlo Prokai. 2011. Isotope-coded dimethyl tagging for differential quantification of posttranslational protein carbonylation by 4-hydroxy-2-nonenal, an end-product of lipid peroxidation. *Journal of Mass Spectrometry* **46**:10, 976-985. [CrossRef]
6. Giancarlo Aldini, Marica Orioli, Marina Carini. 2011. Protein modification by acrolein: Relevance to pathological conditions and inhibition by aldehyde sequestering agents. *Molecular Nutrition & Food Research* n/a-n/a. [CrossRef]
7. Qin Zhu, Zheng Sun, Yue Jiang, Feng Chen, Mingfu Wang. 2011. Acrolein scavengers: Reactivity, mechanism and impact on health. *Molecular Nutrition & Food Research* n/a-n/a. [CrossRef]
8. Yuichiro J. Suzuki , Marina Carini , D. Allan Butterfield . 2010. Protein Carbonylation. *Antioxidants & Redox Signaling* **12**:3, 323-325. [Citation] [Full Text HTML] [Full Text PDF] [Full Text PDF with Links]